



RESEARCH PAPER



## Discovery of a new mitochondria permeability transition pore (mPTP) inhibitor based on gallic acid

José Teixeira<sup>a,b,\*</sup> , Catarina Oliveira<sup>a\*</sup>, Fernando Cagide<sup>a\*</sup>, Ricardo Amorim<sup>a,c,d</sup>, Jorge Garrido<sup>e</sup>, Fernanda Borges<sup>a</sup>  and Paulo J. Oliveira<sup>b</sup> 

<sup>a</sup>CIQUP, Department of Chemistry and Biochemistry, Faculty of Sciences, University of Porto, Porto, Portugal; <sup>b</sup>Center for Neuroscience and Cell Biology, University of Coimbra, UC-Biotech, Cantanhede, Portugal; <sup>c</sup>PhD Programme in Experimental Biology and Biomedicine (PDBEB), Center for Neuroscience and Cell Biology, University of Coimbra, Coimbra, Portugal; <sup>d</sup>III-Institute for Interdisciplinary Research, University of Coimbra, Portugal; <sup>e</sup>Department of Chemical Engineering, School of Engineering (ISEP), Polytechnic Institute of Porto, Porto, Portugal

### ABSTRACT

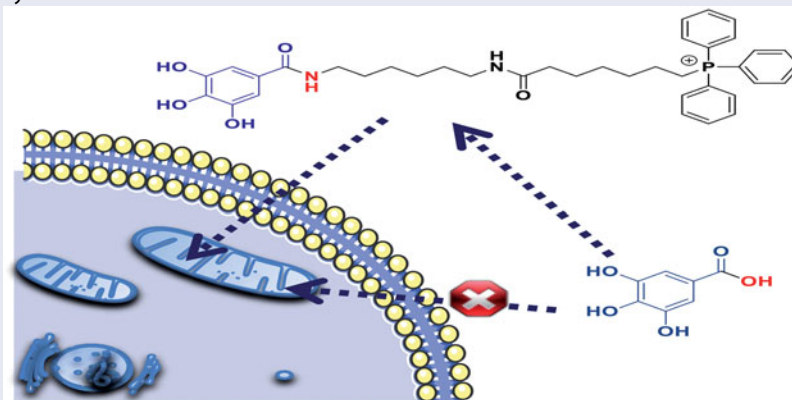
Pharmacological interventions targeting mitochondria present several barriers for a complete efficacy. Therefore, a new mitochondriotropic antioxidant (AntiOxBEN<sub>3</sub>) based on the dietary antioxidant gallic acid was developed. AntiOxBEN<sub>3</sub> accumulated several thousand-fold inside isolated rat liver mitochondria, without causing disruption of the oxidative phosphorylation apparatus, as seen by the unchanged respiratory control ratio, phosphorylation efficiency, and transmembrane electric potential. AntiOxBEN<sub>3</sub> showed also limited toxicity on human hepatocarcinoma cells. Moreover, AntiOxBEN<sub>3</sub> presented robust iron-chelation and antioxidant properties in both isolated liver mitochondria and cultured rat and human cell lines. Along with its low toxicity profile and high antioxidant activity, AntiOxBEN<sub>3</sub> strongly inhibited the calcium-dependent mitochondrial permeability transition pore (mPTP) opening. From our data, AntiOxBEN<sub>3</sub> can be considered as a lead compound for the development of a new class of mPTP inhibitors and be used as mPTP de-sensitiser for basic research or clinical applications or emerge as a therapeutic application in mitochondria dysfunction-related disorders.

### ARTICLE HISTORY

Received 12 December 2017  
Revised 12 February 2018  
Accepted 14 February 2018

### KEYWORDS

Gallic acid;  
mitochondriotropic antioxidant; oxidative stress;  
mitochondrial dysfunction;  
mitochondrial permeability transition pore







### Introduction

Increasing evidence suggests that mitochondrial dysfunction amplifies oxidative stress events playing a crucial role in different pathologies<sup>1–4</sup>. Therefore, mitochondria are attractive targets for several classes of molecules which are aimed to minimise organelle damage, a process involved in the pathophysiology of several diseases. Still, while the role of mitochondria in disease pathogenesis is generally recognised, achieving a targeted therapeutic effect in that organelle is not straightforward<sup>5–7</sup>. Mitochondrial-related diseases treatments are normally focused on maintaining tissue health using preventive measures to mitigate symptom worsening,

such as the optimisation of nutrition and administration of vitamins and food supplements, along with symptom-based management<sup>8–10</sup>.

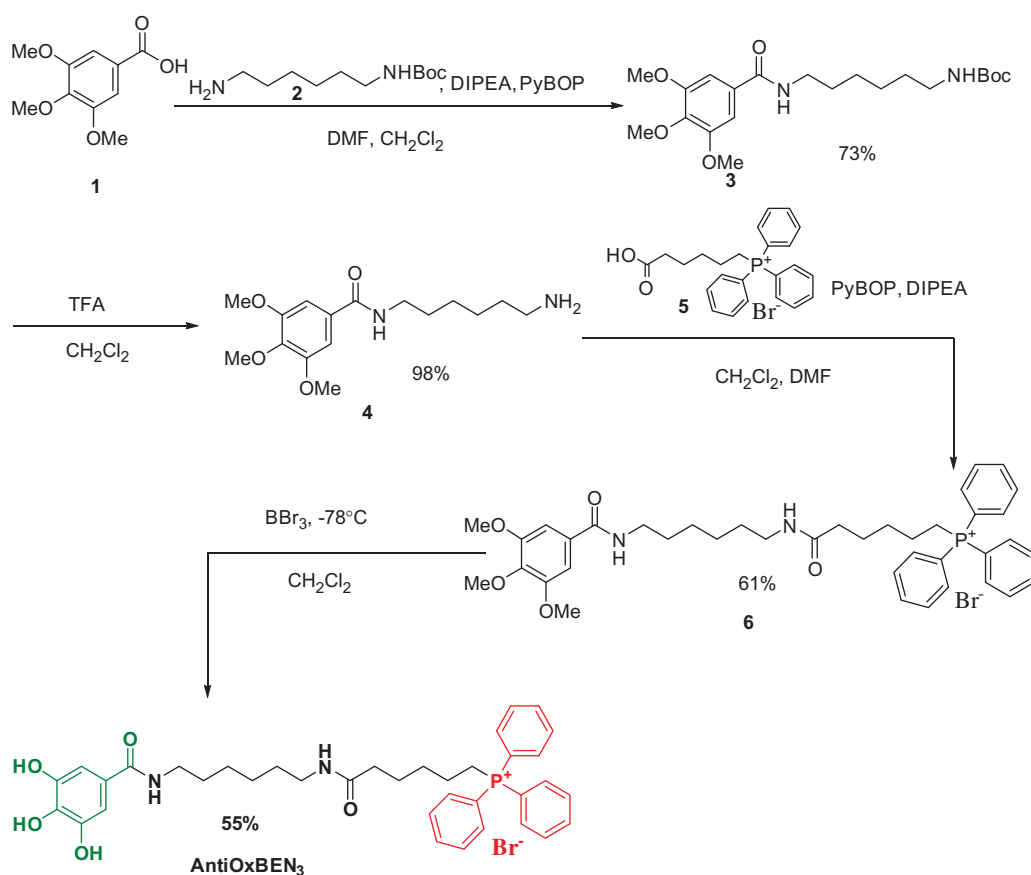
Epidemiological studies and associated meta-analyses suggest that long-term consumption of diets rich in plant polyphenols plays a meaningful role in the prevention and/or avoidance of oxidative-stress related events<sup>11</sup>. Gallic acid (3,4,5-trihydroxybenzoic acid) is a plant phenolic compound widely found in diet. Its antioxidant activity has been associated to its ability to chelate pro-oxidant transition metals (e.g. Cu and Fe), to scavenge radicals by hydrogen donation and/or electron transfer, and to inhibit lipid

**CONTACT** Paulo J. Oliveira  pauloliv@cnc.uc.pt  Center for Neuroscience and Cell Biology, University of Coimbra, UC-Biotech, Biocant Park, Cantanhede 3060197, Portugal; Fernanda Borges  fborges@fc.up.pt  CIQUP/Department of Chemistry and Biochemistry, Faculty of Sciences, University of Porto, Porto 4169007, Portugal

\*These authors contributed equally.

© 2018 The Author(s). Published by Informa UK Limited, trading as Taylor & Francis Group.

This is an Open Access article distributed under the terms of the Creative Commons Attribution License (<http://creativecommons.org/licenses/by/4.0/>), which permits unrestricted use, distribution, and reproduction in any medium, provided the original work is properly cited.



**Scheme 1.** Synthetic strategy pursued for AntiOxBEN<sub>3</sub> development.

peroxidation processes as well as several pro-oxidant enzymes involved in reactive oxygen radical (ROS) production<sup>12,13</sup>.

Although gallic acid is considered to be a versatile antioxidant, its hydrophilic nature restricts its bioavailability and hinders its distribution throughout the body with the inherent difficulties to cross cellular membranes and attain the target sites<sup>12</sup>. The unmet need for new therapies targeting mitochondria stimulates the active search for new agents that can minimise mitochondria dysfunction. Within this framework, a number of mitochondria-targeted therapies have been developed, in particular, those using triphenylphosphonium (TPP) as carrier to deliver molecules to mitochondria<sup>14–16</sup>. Accordingly, it can be anticipated that the development of mitochondriotropic platforms for delivering dietary antioxidants is a rational strategy to prevent mitochondrial oxidative damage.

As part of our long-term project related with the development of more effective antioxidants based on natural models, and guided by the data obtained so far<sup>17,18</sup>, we report here the development of a new mitochondriotropic antioxidant based on gallic acid, named as AntiOxBEN<sub>3</sub> (Scheme 1), with the potential to inhibit the mitochondrial permeability transition.

## Materials and methods

**Reagents, general methods, and apparatus.** All reagents were purchased from Sigma-Aldrich (Barcelona, Spain) and used without additional purification. The solvents were pro-analysis grade and were acquired from Panreac (Lisbon, Portugal) and Sigma-Aldrich. Reaction progress was assessed by thin layer chromatography (TLC) analyses on aluminium silica gel 60 F254 plates (Merck, Darmstadt, Germany) in dichloromethane, ethyl acetate and

dichloromethane/methanol, in several proportions. The spots were detected using UV detection (254 and 366 nm). Flash column chromatography was performed using silica gel 60 (0.040–0.063 mm) (Carlo Erba Reactifs – SDS, Val-de-Reuil, France). Following the workup, solvents were evaporated under reduced pressure in a Buchi Rotavapor (Buchi, New Castle, DE).

<sup>1</sup>H and <sup>13</sup>C spectra NMR spectra were acquired at room temperature and recorded on a Bruker Avance III operating at 400 and 100 MHz, respectively. Chemical shifts are expressed in  $\delta$  (ppm) values relative to tetramethylsilane (TMS) as internal reference and coupling constants (*J*) are given in Hz. Assignments were also made from DEPT (distortionless enhancement by polarisation transfer) (underlined values). Mass spectra (MS) were recorded on a Bruker Microtof (ESI) or Varian 320-MS (EI) apparatus and referred to as *m/z* (% relative) of important fragments.

The purity of the final products (>97% purity) was verified by high-performance liquid chromatography (HPLC) equipped with a UV detector.

## Chemistry

**Synthesis of tert-butyl (6-(3,4,5-trimethoxybenzamido)hexyl)carbamate (3).** 3,4,5-trimethoxybenzoic acid (1, 500 mg, 2.3 mmol) was dissolved in DMF (3.9 ml) at 4 °C and then *N,N*-diethylpropan-2-amine (0.421 ml, 2.3 mmol) and PyBOP (1668 mg, 2.3 mmol) in CH<sub>2</sub>Cl<sub>2</sub> (3.9 ml) were added. The mixture was kept in an ice bath and stirred for half an hour. After this period, tert-butyl (6-amino-hexyl)carbamate (2, 0.529 ml, 2.3 mmol) was added and the mixture was allowed to warm up to room temperature. The reaction was kept with stirring for 18 h. The mixture was then diluted with dichloromethane (20 ml) and washed with saturated NaHCO<sub>3</sub>

solution (2 × 10 ml). The organic phase was dried over Na<sub>2</sub>SO<sub>4</sub>, filtered and concentrated under reduced pressure. The residue was purified by flash chromatography (50% AcOEt/petroleum ether), yield: 73%.

<sup>1</sup>H NMR (400 MHz, CDCl<sub>3</sub>): δ = 7.07 (2H, s, H<sub>5</sub>, H<sub>6</sub>), 6.55 (1H, s, H<sub>1'</sub>), 4.59 (1H, s, H<sub>8'</sub>), 3.91 (6H, s, 2XOCH<sub>3</sub>), 3.88 (3H, s, OCH<sub>3</sub>), 3.43 (2H, dd, *J* = 13.0, 6.9 Hz, H<sub>2'</sub>), 3.13 (1H, dd, *J* = 12.6, 6.2 Hz, H<sub>7'</sub>), 1.67–1.58 (2H, m, H<sub>3'</sub>), 1.53–1.32 (15H, m, H<sub>4'</sub>, H<sub>5'</sub>, H<sub>6'</sub>, NHCOOC(CH<sub>3</sub>)). <sup>13</sup>C NMR (100 MHz, CDCl<sub>3</sub>): δ = 167.3 (CONH), 156.3 (NHCOOC(CH<sub>3</sub>)), 153.3 (C<sub>3</sub>, C<sub>5</sub>), 140.9 (C<sub>4</sub>), 130.4 (C<sub>1</sub>), 104.5 (C<sub>2</sub>, C<sub>6</sub>), 79.3 (NHCOOC(CH<sub>3</sub>)), 61.0 (OCH<sub>3</sub>), 56.4 (2XOCH<sub>3</sub>), 40.0 (C<sub>7'</sub>), 39.7 (C<sub>1'</sub>), 30.2 (C<sub>2'</sub>), 29.5 (C<sub>6'</sub>), 28.5 (NHCOOC(CH<sub>3</sub>)), 26.1 (C<sub>3'</sub>), 25.8 (C<sub>4'</sub>).

**Synthesis of *N*-(6-aminohexyl)-3,4,5-trimethoxybenzamide (4).** The deprotection step was performed adding TFA (4 ml) to a solution of 3 (1 g, 2.4 mmol) in CH<sub>2</sub>Cl<sub>2</sub> (8 ml). The reaction was stirred at room temperature for 1 h. After neutralisation with a saturated NaHCO<sub>3</sub> solution, the organic phase was separated. The organic phase was dried over Na<sub>2</sub>SO<sub>4</sub>, filtered, and concentrated under reduced pressure. The residue was purified by flash chromatography (10% MeOH/CH<sub>2</sub>Cl<sub>2</sub>), yield: 98%.

<sup>1</sup>H NMR (400 MHz, MeOD): δ = 7.19 (2H, s, H<sub>2</sub>, H<sub>6</sub>), 3.89 (6H, s, 2XOCH<sub>3</sub>), 3.80 (3H, s, OCH<sub>3</sub>), 3.39 (1H, t, *J* = 7.1 Hz, H<sub>2</sub>), 2.99–2.90 (2H, m, H<sub>7</sub>), 1.77–1.55 (4H, m, H<sub>3</sub>, H<sub>6</sub>), 1.50–1.36 (4H, m, H<sub>4</sub>, H<sub>5</sub>). <sup>13</sup>C NMR (100 MHz, MeOD): δ = 169.4 (CONH), 154.3 (C<sub>3</sub>, C<sub>5</sub>), 141.8 (C<sub>4'</sub>), 131.1 (C<sub>1</sub>), 105.9 (C<sub>2</sub>, C<sub>6</sub>), 61.2 (OCH<sub>3</sub>), 56.7 (2XOCH<sub>3</sub>), 40.8 (C<sub>7'</sub>), 40.6 (C<sub>1'</sub>), 30.2 (C<sub>6'</sub>), 28.4 (C<sub>3'</sub>), 27.4 (C<sub>4'</sub>), 27.0 (C<sub>5'</sub>).

**Synthesis of [5-(6-(3,4,5-trimethoxybenzamido)hexylamino)carbonylpentyl] triphenylphosphonium bromide (6).** To a solution of compound 4 (689 mg, 2.2 mmol) in DMF (7.4 ml) at 4 °C *N,N*-diethylpropan-2-amine (0.476 ml, 2.7 mmol) and PyBOP (1572 mg, 2.7 mmol) in CH<sub>2</sub>Cl<sub>2</sub> (7.4 ml) were added. The mixture was kept in an ice bath and stirred for half hour. After this period, compound 5 (1218, 2.7 mmol) was added and then the reaction was heated up to room temperature. The reaction was kept under stirring for 20 h. The mixture was then diluted with AcOEt (40 ml) and washed with saturated NaHCO<sub>3</sub> solution (2 × 10 ml). The organic phase was dried over Na<sub>2</sub>SO<sub>4</sub>, filtered and concentrated under reduced pressure. The residue was purified by flash chromatography (10% MeOH/CH<sub>2</sub>Cl<sub>2</sub>), yield: 63%.

<sup>1</sup>H NMR (400 MHz, CDCl<sub>3</sub>): δ = 7.85–7.76 (3H, m, H<sub>4''</sub>), 7.73–7.59 (12H, m, H<sub>2''</sub>, H<sub>3''</sub>, H<sub>5''</sub>, H<sub>6''</sub>), 7.12 (2H, s, H<sub>2</sub>, H<sub>6</sub>), 6.93 (1H, t, *J* = 5.7 Hz, H<sub>1'</sub>), 6.26 (1H, t, *J* = 5.7 Hz, H<sub>8'</sub>), 3.88 (6H, s, 2XOCH<sub>3</sub>), 3.85 (1H, s, OCH<sub>3</sub>), 3.39 (dd, *J* = 13.2, 6.7 Hz, 1H), 3.19–3.05 (4H, m, H<sub>7'</sub>, H<sub>14'</sub>), 2.14 (1H, t, *J* = 7.1 Hz, H<sub>10'</sub>), 1.69–1.26 (14H, m, H<sub>3'</sub>, H<sub>4'</sub>, H<sub>5'</sub>, H<sub>6'</sub>, H<sub>11'</sub>, H<sub>12'</sub>, H<sub>13'</sub>). <sup>13</sup>C NMR (100 MHz, CDCl<sub>3</sub>): δ = 173.3 (C<sub>9'</sub>), 167.2 (PhCONH), 153.1 (C<sub>3</sub>, C<sub>5</sub>), 140.4 (C<sub>4</sub>), 135.4 (d, *J*<sub>CP</sub> = 2.9 Hz, C<sub>4''</sub>), 133.4 (d, *J*<sub>CP</sub> = 9.9 Hz, C<sub>2''</sub>, C<sub>6''</sub>), 130.7 (d, *J*<sub>CP</sub> = 12.6 Hz, C<sub>3''</sub>, C<sub>5''</sub>), 130.4 (C<sub>1</sub>), 117.9 (d, *J*<sub>CP</sub> = 86.2 Hz, C<sub>1''</sub>), 104.5 (C<sub>2</sub>, C<sub>6</sub>), 60.9 (OCH<sub>3</sub>), 56.4 (2XOCH<sub>3</sub>), 39.7 (C<sub>2'</sub>), 39.0 (C<sub>7'</sub>), 36.3 (C<sub>10'</sub>), 30.0 (C<sub>3'</sub>), 29.8 (C<sub>6'</sub>), 28.9 (d, *J* = 5.0 Hz, C<sub>12'</sub>), 26.6 (C<sub>4'</sub>), 25.9 (C<sub>5'</sub>), 24.9 (C<sub>11'</sub>), 22.3 (d, *J* = 43.5 Hz, C<sub>14'</sub>), 22.1 (d, *J* = 12.5 Hz, C<sub>13'</sub>).

**Synthesis of [5-(6-(3,4,5-trihydroxybenzamido)hexylamino) carbonylpentyl]triphenylphosphonium bromide (AntiOxBEN<sub>3</sub>).** Compound 6 (1.0 g; 1.4 mmol) was dissolved in 7.6 ml of anhydrous dichloromethane. The reaction mixture was stirred under argon and cooled at a temperature below –75 °C. Boron tribromide (4.3 ml of 1 M solution in dichloromethane; 4.3 mmol) solution was added dropwise and the reaction was kept at –75 °C for 10 min. Once the addition was completed, the reaction was kept at –70 °C for 10 min and then allowed to warm to room temperature with continuous stirring for 12 h. Thereafter, the reaction was finished by slow addition of water (20 ml). After water removal, the resulting product

was dissolved in methanol and dried over anhydrous Na<sub>2</sub>SO<sub>4</sub>, filtered, and the solvent evaporated. The residue was purified by flash chromatography (10% MeOH/CH<sub>2</sub>Cl<sub>2</sub>), yield: 55%.

<sup>1</sup>H NMR (400 MHz, MeOD): δ = 7.92–7.83 (3H, m, H<sub>4''</sub>), 7.82–7.70 (12H, m, 12H, m, H<sub>2''</sub>, H<sub>3''</sub>, H<sub>5''</sub>, H<sub>6''</sub>), 6.83 (2H, s, H<sub>2</sub>, H<sub>6</sub>), 3.43–3.34 (2H, m, H<sub>14'</sub>), 3.33–3.25 (2H, m, H<sub>2'</sub>), 3.14 (1H, t, *J* = 6.9 Hz, H<sub>7'</sub>), 2.15 (1H, t, *J* = 7.0 Hz, H<sub>10'</sub>), 1.72–1.28 (14H, m, H<sub>3'</sub>, H<sub>4'</sub>, H<sub>5'</sub>, H<sub>6'</sub>, H<sub>11'</sub>, H<sub>12'</sub>, H<sub>13'</sub>). <sup>13</sup>C NMR (100 MHz, MeOD): δ = 176.3 (C<sub>9</sub>), 170.5 (PhCOONH), 146.5 (C<sub>3</sub>, C<sub>5</sub>), 138.1 (C<sub>4</sub>), 136.1 (d, *J* = 2.9 Hz, C<sub>4''</sub>), 134.7 (d, *J*<sub>CP</sub> = 10.0 Hz, C<sub>2''</sub>, C<sub>6''</sub>), 131.5 (d, *J*<sub>CP</sub> = 12.6 Hz, C<sub>3''</sub>, C<sub>4''</sub>), 125.4 (C<sub>1</sub>), 119.7 (d, *J*<sub>CP</sub> = 86.3 Hz, C<sub>1''</sub>), 107.8 (C<sub>2</sub>, C<sub>6</sub>), 40.8 (C<sub>2'</sub>), 40.5 (C<sub>7'</sub>), 36.2 (C<sub>10'</sub>), 30.9 (C<sub>3'</sub>), 30.8 (C<sub>6'</sub>), 30.2 (C<sub>4'</sub>), 29.9 (C<sub>5'</sub>), 27.4 (d, *J*<sub>CP</sub> = 2.5 Hz, C<sub>12'</sub>), 26.1 (C<sub>11'</sub>), 23.1 (d, *J*<sub>CP</sub> = 4.2 Hz, C<sub>13'</sub>), 22.6 (d, *J*<sub>CP</sub> = 51.3 Hz, C<sub>14'</sub>). ESI/MS *m/z* (%): 628 (M<sup>+</sup>+H-Br<sup>-</sup>, 38), 627 (M<sup>+</sup>-Br, 100), 556 (35), 547 (46). ESI/HRMS *m/z* calc. for C<sub>37</sub>H<sub>44</sub>N<sub>2</sub>O<sub>5</sub>P<sup>+</sup> (M<sup>+</sup>-Br<sup>-</sup>): 627.2982; found 627.2970.

## Pharmacology

### Evaluation of AntiOxBEN<sub>3</sub> functional mitochondrial toxicity profile

**Animals.** Male Wistar Han rats (10 weeks old) were housed in our accredited animal colony (Laboratory Research Center, Faculty of Medicine of University of Coimbra, Coimbra, Portugal). Animals were group-housed in type III-H cages (Tecniplast, Varese, Italy) and maintained in specific environmental requirements (22 °C, 45–65% humidity, 15–20 changes/hour ventilation, 12 h artificial light/dark cycle, noise level <55 dB) and with free access to standard rodent food (4RF21 GLP certificate, Mucedola, Settimo Milanese, Italy) and acidified water (at pH 2.6 with HCl to avoid bacterial contamination). The research procedure was carried out in accordance with European Requirements for Vertebrate Animal Research and approved by the animal welfare committee of the Center for Neuroscience and Cell Biology, University of Coimbra, Coimbra, Portugal. Further approval was obtained from the National Agency for Veterinary and Agriculture (DGAV), reference 0421/000/000/2016.

**Isolation of rat liver mitochondria.** Rat liver mitochondria (RLM) were prepared by tissue homogenisation followed by differential centrifugations in ice-cold buffer containing 250 mM sucrose, 10 mM HEPES (pH 7.4), 1 mM EGTA, and 0.1% fat-free bovine serum albumin<sup>19</sup>. After obtaining a crude mitochondrial preparation, pellets were washed twice and resuspended in washing buffer (250 mM sucrose and 10 mM HEPES, pH 7.4). Mitochondrial protein concentration was determined by the biuret assay using BSA (bovine serum albumin) as a standard<sup>20</sup>.

**Measurement of AntiOxBEN<sub>3</sub> mitochondrial uptake.** The uptake of AntiOxBEN<sub>3</sub> by energised RLM was evaluated by using an ion-selective electrode, according to previously established methods, which measures the distribution of tetraphenylphosphonium (TPP<sup>+</sup>). An Ag/AgCl<sub>2</sub> electrode was used as reference. To measure AntiOxBEN<sub>3</sub> uptake, RLM (0.5 mg protein/ml) were incubated with constant stirring, at 37 °C, in 1 ml of KCl medium (120 mM KCl, 10 mM HEPES, pH 7.2, and 1 mM EGTA). Five sequential 1 μM additions of AntiOxBEN<sub>3</sub> were performed to calibrate the electrode response in the presence of rotenone (1.5 μM). Then succinate (10 mM) was added to generate ΔΨ and valinomycin (0.2 μg/ml) was added at the end of the experiment to dissipate ΔΨ. The mitochondrial accumulation ratio was calculated by the disappearance of AntiOxBEN<sub>3</sub> from extra- to intramitochondrial medium assuming an intramitochondrial volume of 0.5 μl/mg protein and

a binding correction expected for the mitochondrial uptake of TPP compounds<sup>21</sup>.

**Evaluation of AntiOxBEN<sub>3</sub> effect on mitochondrial respiration.** Isolated RLM oxygen consumption was evaluated polarographically with a Clark-type oxygen electrode, connected to a suitable recorder in a 1 ml thermostated water-jacketed chamber with magnetic stirring, at 37 °C. The standard respiratory medium consisted of 130 mM sucrose, 50 mM KCl, 5 mM KH<sub>2</sub>PO<sub>4</sub>, 5 mM HEPES (pH 7.3), and 10 μM EGTA. Increasing concentrations of AntiOxBEN<sub>3</sub> (2.5–10 μM) were added to the reaction medium containing respiratory substrates glutamate/malate (10 and 5 mM, respectively) or succinate (5 mM) and RLM (1 mg) and allowed to incubate for a 5 min period prior to initiate the registration. State 2 was measured as the oxygen consumption measured during the 5 min incubation time with AntiOxBEN<sub>3</sub>. To induce state 3 respiration, 125 nmol ADP (when using glutamate/malate) or 75 nmol ADP (when using succinate) was added. State 4 was determined after cessation of ADP phosphorylation. Subsequent addition of oligomycin (2 μg/ml) inhibited ATP-synthase and resulted in oligomycin-resistant respiration. Finally, 1 μM FCCP was added to uncouple respiration. The presented results are means ± SEM of seven independent experiments.

**Evaluation of AntiOxBEN<sub>3</sub> effect on mitochondrial transmembrane electric potential (ΔΨ).** Approximate values for mitochondrial transmembrane electric potential (ΔΨ) was estimated through the evaluation of fluorescence changes of safranin O (5 μM) and was recorded on a spectrofluorometer operating at excitation and emission wavelengths of 495 and 586 nm, with a slit width of 5 nm. Increasing concentrations of AntiOxBEN<sub>3</sub> (2.5–10 μM) were added to the reaction medium (200 mM sucrose, 1 mM KH<sub>2</sub>PO<sub>4</sub>, 10 mM Tris (pH 7.4), and 10 μM EGTA) containing respiratory substrates glutamate/malate (5 and 2.5 mM, respectively) or succinate (5 mM) and RLM (0.5 mg in 2 ml final volume) and allowed to incubate for a 5 min period prior to recording, at 25 °C. In this assay, safranin (5 μM) and ADP (25 nmol) were used to initiate the assay and to induce depolarisation, respectively. Moreover, 1 μM FCCP was added at the end of all experiments to cause complete mitochondrial depolarisation. ΔΨ was calculated using a calibration curve obtained when RLM were incubated in a reaction medium mostly devoid of K<sup>+</sup>, containing 200 mM sucrose, 1 mM NaH<sub>2</sub>PO<sub>4</sub>, 10 mM Tris (pH 7.4), and 10 μM EGTA, supplemented with 0.4 μg valinomycin, as previous described<sup>22,23</sup>. The extension of fluorescence changes of safranin induced by ΔΨ was found to be similar in the standard and K<sup>+</sup>-free medium. "Repolarisation" corresponds to the recovery of apparent ΔΨ after the complete phosphorylation of ADP added. Lag phase reflects the time required to phosphorylate the added ADP. Values are means ± SEM of five independent experiments.

**Evaluation of AntiOxBEN<sub>3</sub> iron chelating properties.** The assay was performed in ammonium acetate buffer (pH 6.7) using a solution of ammonium iron (II) sulphate in ammonium acetate as the source of ferrous ions. In each well, a solution of the test compound (100 μM) and ammonium iron (II) sulphate in ammonium acetate (20 μM) was added, incubated for 10 min and the absorbance read at 562 nm. An aqueous 5 mM solution of ferrozine was freshly prepared and then added to each well (96 μM final concentrations). After a new incubation at 37 °C during 10 min, the absorbance of [Fe(ferrozine)<sub>3</sub>]<sup>2+</sup> complex was measured at 562 nm. EDTA was used as a reference. All compounds, including ferrozine, were tested at the final concentration of 100 μM. The absorbance of the first reading was subtracted from the final values to discard any absorbance due to the test compounds. Data are means ± SEM of three independent experiments and are expressed as Δabsorbance at 562 nm.

**Evaluation of AntiOxBEN<sub>3</sub> effect on RLM lipid peroxidation.** The effect of AntiOxBEN<sub>3</sub> on RLM lipid peroxidation was evaluated by measuring thiobarbituric acid reactive species (TBARS). RLM (2 mg protein/ml) were incubated in 0.8 ml medium containing 100 mM KCl, 10 mM Tris-HCl and pH 7.6, at 37 °C, supplemented with 5 mM glutamate/2.5 mM malate as substrates. RLM was incubated for a 5 min period with the different tested compounds (5 μM) after which mitochondria were exposed to oxidative stress condition by the addition of 100 μM FeSO<sub>4</sub>/500 μM H<sub>2</sub>O<sub>2</sub>/5 mM ascorbate for 15 min at 37 °C. After exposure to oxidative stress, 60 μl of 2% (v/v) butylated hydroxytoluene in DMSO was added, followed by 200 μl of 35% (v/v) perchloric acid and 200 μl of 1% (w/v) thiobarbituric acid. Samples were then incubated for 15 min at 100 °C, allowed to cool down and the supernatant transferred to a glass tube. After addition of 2 ml MilliQ water and 2 ml butan-1-ol, samples were vigorously vortexed for few seconds. The two phases were allowed to separate. The fluorescence of aliquots (250 μl) of the organic layer was analysed in a plate reader (λEx = 515 nm; λEm = 553 nm) for TBARS. Data are means ± SEM of three independent experiments and are expressed as % of control (control = 100%).

**Evaluation of AntiOxBEN<sub>3</sub> effect on mitochondrial permeability transition pore opening.** Mitochondrial swelling was estimated by alterations of the light scattered from the mitochondrial suspension, increasing concentrations of AntiOxBEN<sub>3</sub> (2.5–10 μM) was added to the reaction medium (200 mM sucrose, 1 mM KH<sub>2</sub>PO<sub>4</sub>, 10 mM Tris (pH 7.4), 5 mM succinate and 10 μM EGTA supplemented with 1.5 μM rotenone) in the presence of RLM (1 mg) and allowed to incubate for a 5 min period prior to initiating the recording. The experiments were started by the addition of a suitable concentration of Ca<sup>2+</sup> (15–50 μM), determined every day, and the absorbance at 540 nm monitored every minute for a 15 min period. Cyclosporin A (CSA) (1 μM), a mPTP de-sensitiser<sup>24</sup>, was added to confirm mPTP opening. The reaction was stirred continuously and the temperature maintained at 37 °C. Data are means ± SEM of three independent experiments and are expressed as Δabsorbance at 540 nm.

### **Evaluation of AntiOxBEN<sub>3</sub> cytotoxic and antioxidant cellular profile**

**Cell culture conditions.** Hepatocellular carcinoma HepG2 cells (ECACC, Salisbury, UK) were cultured in high-glucose medium composed by Dulbecco's modified Eagle's medium (DMEM; D5648) supplemented with sodium pyruvate (0.11 g/l), sodium bicarbonate (1.8 g/l) and 10% foetal bovine serum (FBS) and 1% of antibiotic penicillin-streptomycin 100 × solution. Cells were maintained at 37 °C in a humidified incubator with 5% CO<sub>2</sub>.

**Cytotoxicity screening using sulforhodamine B assay.** After the treatment period, the sulforhodamine B (SRB) assay was used for cell mass determination, which is based on the measurement of cellular protein content. Briefly, after compound incubation, the medium was removed and wells rinsed with PBS (1X). Cells were fixed by adding 1% acetic acid in 100% methanol for at least 2 h at –20 °C. Then, this solution was discarded and the plates dried in an oven at 37 °C. Two hundred and fifty μl of 0.5% SRB in 1% acetic acid solution was added and incubated at 37 °C for 1 h. The wells were then washed to remove the excess of the dye with 1% acetic acid and dried. Then, 500 μl of Tris (pH 10) was added and the plates were stirred for 15 min. Finally, 200 μl of each supernatant was transferred in 96-well plates and optical density was measured at 540 nm.

**Antioxidant protective effect.** Cells were placed on 48-well plate ( $4 \times 10^4$  cells/ml), cultured for 24 h before treatment and then were pre-incubated with AntiOxBEN<sub>3</sub> (100  $\mu$ M), a concentration in which cell mass was not affected, for 1 h. Cells were then exposed to oxidative stress by the addition of 250  $\mu$ M FeSO<sub>4</sub> or 250  $\mu$ M H<sub>2</sub>O<sub>2</sub> for 48 h. At the end of treatment time, the SRB assay was used for cell mass determination. Data are means  $\pm$  SEM of six independent experiments and are expressed as percentage of control, which represents the cell mass without any treatment in the respective time point.

### Statistics

GraphPad Prism version 5.0 software (GraphPad Software, Inc., La Jolla, CA) was used for data analysis. All results were expressed as means  $\pm$  SEM for the number of assays indicated in each experiment. Data were analysed by the student's t-test for comparison of two means, and one-way ANOVA with Dunnett multiple comparison post-test to compare groups with one independent variable. Significance was accepted with \* $p < .05$ , \*\* $p < .01$ , \*\*\* $p < .0005$ , \*\*\*\* $p < .0001$ .

### Results and discussion

Research on mitochondriotropic antioxidants has been increasing over the last years. One viable and promising strategy involves the use of dietary polyphenolic antioxidants templates along with the chemical modulation of their properties, including mitochondrial targeting ability, efficacy, and toxicity<sup>25</sup>. In this context, some mitochondria-targeted polyphenolic-based molecules have been developed including MitoResveratrol, MitoCurcumin, and MitoQuercetin<sup>26–28</sup>. Despite the described antioxidant properties of the parent polyphenols, the new mitochondria-targeted derivatives have been shown to destabilise mitochondrial function exhibiting antiproliferative effects on different cell models, namely tumour cells<sup>29–31</sup>. Still, these works clearly show that mitochondrial targeting of polyphenols can be achieved, although in a disease context it is desirable that mitochondrial protection, and no toxicity, is attained.

In order to generate a mitochondria-targeted gallic acid derivative with cytoprotective activity, AntiOxBEN<sub>3</sub> was generated as a tripartite entity having as a cap the gallic moiety, a peptide-like flexible spacer, and TPP as the ending group (Scheme 1). AntiOxBEN<sub>3</sub> was synthesised following a four-step strategy in which trimethoxybenzoic acid 1 was linked to a monoprotected diamine 2 spacer to obtain the derivative 3. Compound 4 was obtained from compound 3 by a deprotection process in acid medium. Amine 4 was then coupled to the TPP cationic compound 5 by an amidation reaction in which the acylating agent was generated *in situ*. Then, compound 6 was demethylated using tribromide (BBr<sub>3</sub>) solution to obtain AntiOxBEN<sub>3</sub>. Globally, good to moderate yields have been obtained.

#### AntiOxBEN<sub>3</sub> mitochondrial uptake and functional mitochondrial toxicity profile

The next step was to evaluate AntiOxBEN<sub>3</sub> mitochondrial uptake by measuring its accumulation in isolated RLM in response to the membrane electric potential ( $\Delta\Psi$ )<sup>32</sup>. In the presence of rotenone,  $\Delta\Psi$  was generated by the addition of Complex II substrate succinate (10 mM), leading to a decrease in the extramitochondrial compound concentration. The accumulated AntiOxBEN<sub>3</sub> was extruded from mitochondria once  $\Delta\Psi$  was abolished by the K<sup>+</sup>-ionophore

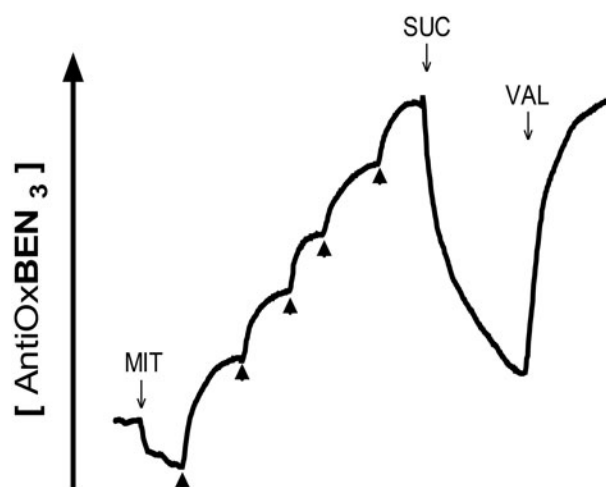


**Figure 1.** AntiOxBEN<sub>3</sub> uptake by energised rat liver mitochondria measured using a TPP-selective electrode. MIT, mitochondria; SUC, succinate; VAL, valinomycin.

valinomycin (VAL) (Figure 1). The  $\Delta\Psi$  generated by RLM resulted into accumulation of approximately 5000-fold within the mitochondrial matrix. Similarly to other lipophilic antioxidants containing a TPP cation<sup>17,18,21</sup>, AntiOxBEN<sub>3</sub> was able to penetrate in mitochondria driven by the  $\Delta\Psi$ , accumulating up to several hundred-fold, increasing significantly the concentration and potency of the targeted compound.

Isolated rat hepatic mitochondrial fractions were also used to detect direct toxic effects of AntiOxBEN<sub>3</sub> on the bioenergetics apparatus. Similarly to previous studies<sup>17,18</sup>, the effect of AntiOxBEN<sub>3</sub> on mitochondrial bioenergetic apparatus was evaluated at three different concentrations (2.5, 5, and 10  $\mu$ M) by measuring O<sub>2</sub> consumption and approximate  $\Delta\Psi$ . In addition, mitochondrial functionality parameters (RCR, respiratory control ratio and ADP/O ratio, which measure the ADP phosphorylation efficiency) were evaluated.

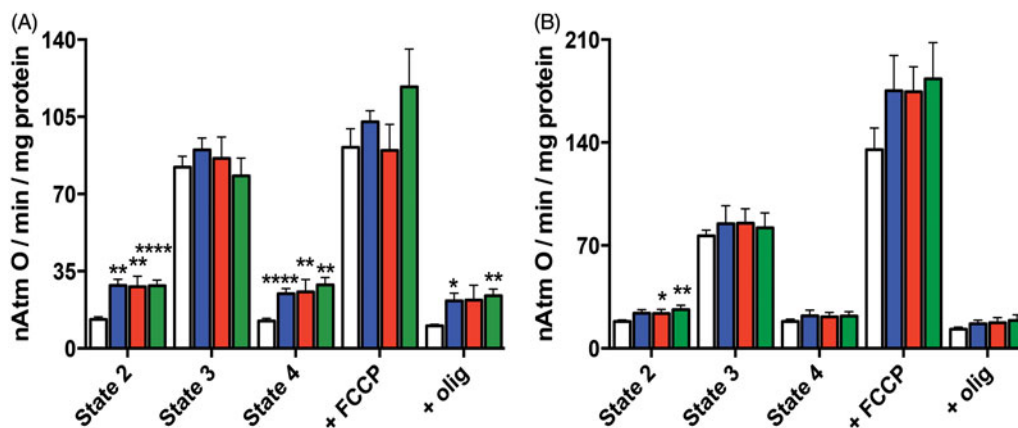
Hepatic mitochondrial fractions were energised with Complex I or Complex II substrates, developing an apparent  $\Delta\Psi \approx 230$  mV or  $\approx 186$  mV (negative inside), during glutamate/malate- and succinate-energisation, respectively (Table 1). Despite AntiOxBEN<sub>3</sub> mitochondriotropic mechanism, it is important to note that the alterations caused by the compound on the  $\Delta\Psi$  values measured were not statistically significant.

Hepatic mitochondrial fractions were similarly energised in order to detect direct effects of AntiOxBEN<sub>3</sub> on mitochondrial O<sub>2</sub> consumption. Respiratory rates characteristic of state 2, state 3, state 4, oligomycin-resistant respiration and FCCP-stimulated respiration are shown in Figure 2. The respiratory control ratio (RCR, state 3/state 4 respiration), which gives insight on oxidative phosphorylation coupling, was of  $7.3 \pm 0.6$  and  $4.1 \pm 0.3$  for the control experiments when glutamate-malate and succinate were used as respiratory substrates, respectively. ADP/O was  $2.6 \pm 0.1$  and  $1.5 \pm 0.1$  when glutamate-malate and succinate, respectively, were used as respiratory substrates (Table 1). Although AntiOxBEN<sub>3</sub>-induced alterations on mitochondrial respiration supported by the two substrates followed the same general tendency, these changes were more pronounced when Complex I substrates were used. AntiOxBEN<sub>3</sub> caused a concentration-dependent marked increase in state 2, state 4 and oligomycin-resistant respiration (Figure 2). The overall consequence was a significant decrease in the RCR. The ADP/O was also significantly affected with 10  $\mu$ M AntiOxBEN<sub>3</sub> (Table 1). This new mitochondriotropic agent appeared to increase the mitochondrial inner membrane permeability to protons, or to other cations, a process

**Table 1.** Effect of AntiOxBEN<sub>3</sub> on mitochondrial bioenergetics: mitochondrial respiratory control ratio (RCR); ADP phosphorylation efficiency (ADP/O); and approximate transmembrane electric potential ( $\Delta\Psi$ ).

Mitochondrial Bioenergetics		Control	AntiOxBEN <sub>3</sub>		
			2.5 $\mu$ M	5 $\mu$ M	10 $\mu$ M
Glut/Mal	Maximum potential (app. $\Delta\Psi$ in – mV)	229.8 $\pm$ 17.4	221.1 $\pm$ 20.2	221.4 $\pm$ 22.6	227.5 $\pm$ 26.3
	RCR	7.3 $\pm$ 0.6	3.9 $\pm$ 0.5**	3.9 $\pm$ 0.6**	3.07 $\pm$ 0.6****
	ADP/O	2.6 $\pm$ 0.1	2.3 $\pm$ 0.2	2.3 $\pm$ 0.1	2.0 $\pm$ 0.2*
Succinate	Maximum potential (app. $\Delta\Psi$ in – mV)	186.1 $\pm$ 6.6	203.6 $\pm$ 16.6	205.3 $\pm$ 19.4	207.9 $\pm$ 19.3
	RCR	4.1 $\pm$ 0.3	4.1 $\pm$ 0.5	4.3 $\pm$ 0.7	3.9 $\pm$ 0.4
	ADP/O	1.5 $\pm$ 0.1	1.6 $\pm$ 0.1	1.6 $\pm$ 0.1	1.7 $\pm$ 0.1

Effect of AntiOxBEN<sub>3</sub> on approximate  $\Delta\Psi$ , RCR and ADP/O of energised RLM (5 mM glutamate/2.5 malate or 5 mM succinate). Values are means  $\pm$  SEM of five independent experiments. Statistically significant compared with control using Student's two tailed t-test. Significance was accepted with \* $p$  < .05, \*\* $p$  < .01, \*\*\*\* $p$  < .0001.

**Figure 2.** Effect of AntiOxBEN<sub>3</sub> on RLM respiration supported by (A) 10 mM glutamate + 5 mM malate or (B) 5 mM succinate. The white bars refer to control, while blue, red and green bars refer to experiments where RLM were pre-incubated with AntiOxBEN<sub>3</sub> (2.5, 5, and 10  $\mu$ M, respectively). Olig, oligomycin. The presented results are means  $\pm$  SEM of seven independent experiments. \* $p$  < .05, \*\* $p$  < .01, \*\*\*\* $p$  < .0001 vs. control.

that may occur through the induction of a membrane disturbance. Although several mitochondria-targeted rhodamine cationic derivatives presented uncoupling effect<sup>33</sup>, our data argue against a protonophoretic activity exerted by AntiOxBEN<sub>3</sub>, since this mitochondria-targeted antioxidant had a negligible effect on the apparent  $\Delta\Psi$  measured (Table 1). These types of compounds have a strong tendency to adsorb as a monolayer onto the surface of phospholipid bilayers and the TPP component is always found at the same position in the potential energy well on the membrane surface, whereas the hydrophobic alkyl chain is usually inserted into the hydrophobic core of the membrane. Moreover, the high volume of matrix-facing mitochondrial membrane relative to that of the matrix means that a very large proportion of the TPP cation within mitochondria is membrane-bound<sup>7</sup>, which may explain the increase of mitochondrial inner membrane permeability to protons.

Mitochondria-targeted antioxidants containing the TPP<sup>+</sup> moiety can freely pass through cellular phospholipid bilayers, with the extent of anchoring being mainly dependent upon their hydrophobicity. Consequently, it is somehow expected that AntiOxBEN<sub>3</sub> would exhibit similar cytotoxicity towards hepatocarcinoma cells as another type of mitochondriotropic hydroxybenzoic acid derivatives<sup>34,35</sup>. Surprisingly, AntiOxBEN<sub>3</sub> was less toxic regarding mitochondrial functional end-points in isolated liver fractions in the same range of concentrations tested, meaning that the type (ester vs. amide) and length of the linker may also play a role on hydroxybenzoic acid derivatives induced-toxicity. Recent works showing targeting of different polyphenols to mitochondria reported that their mechanism of action involves the destabilisation of  $\Delta\Psi$  and consequent induction of mPTP opening<sup>34,36</sup>. Although AntiOxBEN<sub>3</sub> also addressed gallic acid to mitochondria, antioxidant properties

of the precursor were maintained and mitochondrial function was not visibly affected, which is clearly an advantage over these recent works.

#### AntiOxBEN<sub>3</sub> iron chelation properties

As iron overload and loss of iron homeostasis are associated with oxidative stress<sup>37</sup>, and ultimately to mitochondrial dysfunction, the AntiOxBEN<sub>3</sub> iron chelating properties were evaluated. Data show that AntiOxBEN<sub>3</sub> can chelate ferrous iron, as observed for the significant decrease in [Fe(ferrozine)]<sub>2</sub><sup>+</sup> complex formation. Still, EDTA, a well-known metal chelator, was the best chelating agent tested (Figure 3(A)), as the binding constant of EDTA for its complex with iron is higher than that of phenolic acids<sup>38</sup>. Most important, the TPP cation and the alkyl spacer did not have a relevant effect on AntiOxBEN<sub>3</sub> chelation properties, when compared to gallic acid alone. AntiOxBEN<sub>3</sub> metal chelation properties, which are similar to that presented by gallic acid, can be ascribed to the presence of the pyrogallol system and are likely involved in their antioxidant mechanism. As, gallic type systems have intrinsic metal chelating properties<sup>39</sup>, and this motif was not altered in AntiOxBEN<sub>3</sub>, one can consider that it is the moiety responsible for the observed iron chelation and antioxidant activities.

#### AntiOxBEN<sub>3</sub> effects on lipid peroxidation

The enrichment of mitochondrial membranes in polyunsaturated fatty acids, and their proximity to ROS production sites, makes mitochondria particularly vulnerable to lipid peroxidation. Therefore, the antioxidant action of AntiOxBEN<sub>3</sub> antagonising lipid

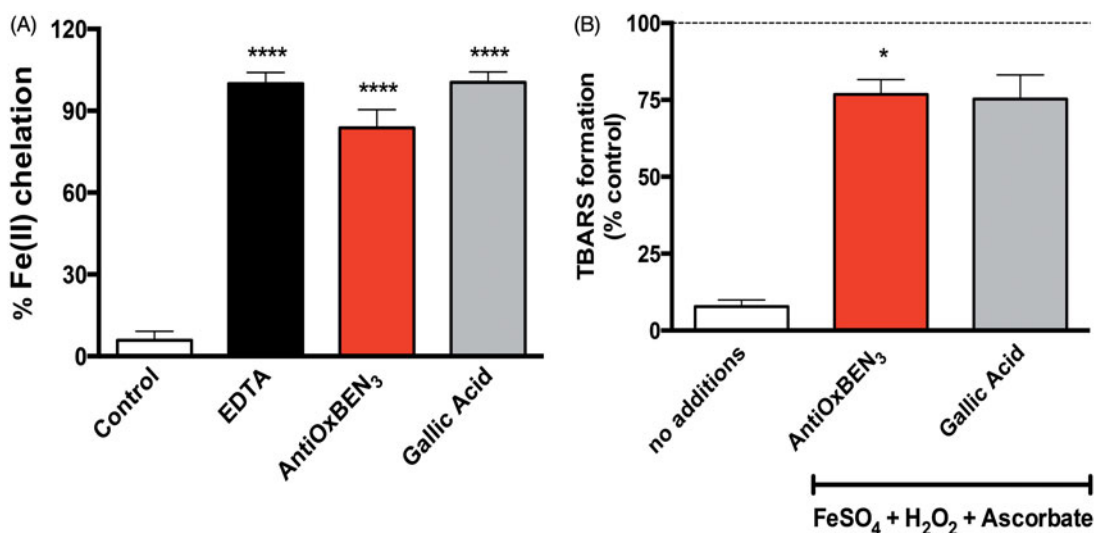


**Figure 3.** AntiOxBEN<sub>3</sub> antioxidant properties. (A) AntiOxBEN<sub>3</sub> iron chelation properties, EDTA (chelating agent) was used as reference. Data are means  $\pm$  SEM from three independent experiments and are expressed as % of Fe(II) chelation. (B) AntiOxBEN<sub>3</sub> effect on mitochondrial lipid peroxidation. Data are means  $\pm$  SEM from three independent experiments and are expressed as % of control. \*\*\*\* $p$  < .0001 vs. control (A), \* $p$  < .05 vs. no additions (B).

peroxidation was evaluated. AntiOxBEN<sub>3</sub> prevented lipid peroxidation stimulated by H<sub>2</sub>O<sub>2</sub>/FeSO<sub>4</sub>/ascorbate system, assessed as TBARS production in RLM (Figure 3(B)). Similarly to gallic acid, that prevents lipid peroxidation due to its antioxidant and anti-lipoperoxidative properties<sup>40,41</sup>, AntiOxBEN<sub>3</sub> prevented lipid peroxidation likely through its direct radical scavenging activity, although its direct iron-chelation properties cannot be discarded. In fact, AntiOxBEN<sub>3</sub> can chelate the ferrous iron present in solution, which is maintained in this form by the presence of ascorbate in the oxidative system.

#### AntiOxBEN<sub>3</sub> effects on mitochondrial permeability transition pore

Mitochondrial permeability transition pore (mPTP) opening is usually linked to mitochondrial dysfunction, as it results in a solute exchange between mitochondrial matrix contents and the surrounding cytoplasm, and is connected to mitochondrial depolarisation, cessation of ATP synthesis, Ca<sup>2+</sup> release, pyridine nucleotide depletion, inhibition of respiration and ultimately to organelle swelling and membrane rupture<sup>42</sup>. mPTP opening is involved in the toxicity process of different xenobiotics<sup>43,44</sup> and in different pathologies, which ultimately result in cell damage and death<sup>45,46</sup>.

As mPTP opening can be induced, among other factors, by calcium (Ca<sup>2+</sup>) overload and excessive ROS production, we evaluated AntiOxBEN<sub>3</sub> effects on calcium-induced mPTP opening. CsA, a mPTP de-sensitiser<sup>24</sup>, was added to confirm that the mitochondrial swelling observed resulted from mPTP induction. Remarkably, for all AntiOxBEN<sub>3</sub> tested concentrations, no mPTP inducing effect was observed. In opposition, AntiOxBEN<sub>3</sub> showed concentration-dependent inhibitory effects (Figure 4) similarly to CsA. Increased mitochondrial membrane permeability due to opening of the mPTP may be greatly enhanced by adenine nucleotide depletion, calcium influx, elevated phosphate, and oxidative stress<sup>47</sup>. AntiOxBEN<sub>3</sub> protective effects may be related with its antioxidant activity, interference with one of the mPTP components or through the chelation of calcium ions. The capability of gallic acid chelate zinc, calcium, and magnesium metals and the stability of such complexes confirmed the evidence that phenolic chelators

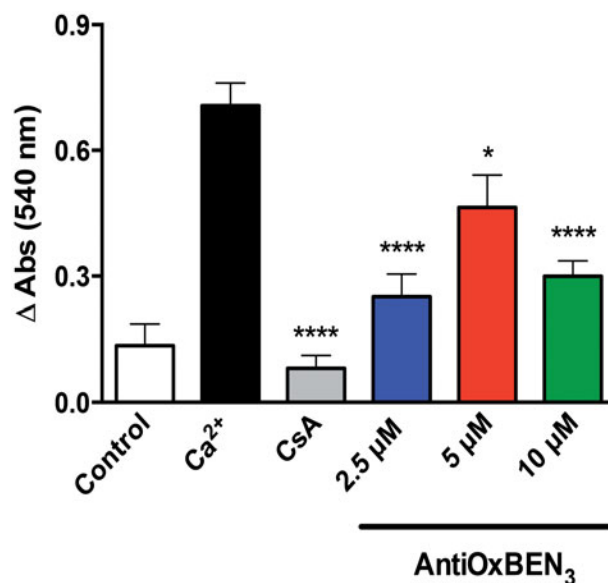


**Figure 4.** AntiOxBEN<sub>3</sub> effects on mitochondrial swelling resulting from induction of the mitochondrial permeability transition pore (mPTP) opening. Data are means  $\pm$  SEM from three independent experiments and are expressed as  $\Delta$ absorbance at 540 nm. \* $p$  < .05, \*\*\*\* $p$  < .0001 vs. Ca<sup>2+</sup>.

possess chelating power either for mono and divalent metals<sup>48</sup>, although it is possible that in our present case, and based on the stoichiometry of the complexation reactions, some free calcium may still be available. Recently, it was demonstrated that gallic acid prevented mitochondrial swelling induced by different stimuli independent of calcium overload, suggesting that it act as a genuine inhibitor of mPTP and not by affecting mitochondrial calcium loading<sup>49</sup>. The ATP synthase has recently been proposed as the molecular component of the mPTP<sup>42</sup>. Inhibitory effects of some polyphenols on the ATP synthetase/ATPase activities were extensively reviewed<sup>50,51</sup>. Although catechin gallates (flavonoid esters of gallic acid) were mentioned, no references to gallic acid is mentioned. In a far-stretch assumption, Nanjundiah et al. reported the gastroprotective effect of ginger rhizome, mainly due to the

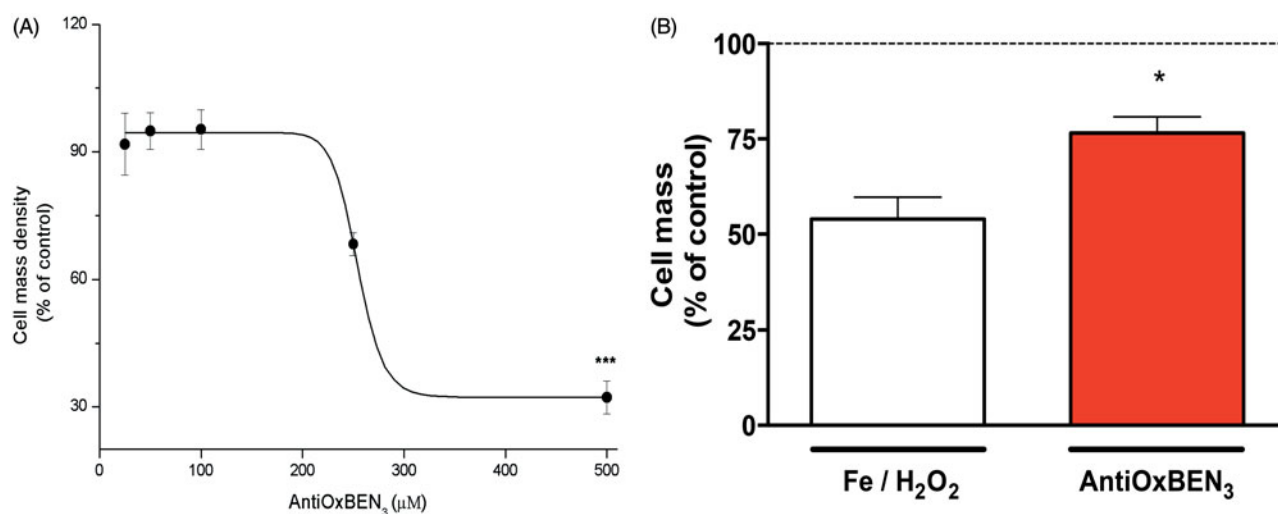


**Figure 5.** AntiOxBEN<sub>3</sub> cytotoxicity and antioxidant outline on human hepatocellular carcinoma cells (HepG2). (A) Cytotoxicity profile on HepG2. (B) Antioxidant profile on HepG2 using iron and hydrogen peroxide as oxidant stressors. Data are means  $\pm$  SEM from five independent experiments and are expressed as % of control. \* $p < .05$  vs. Fe/H<sub>2</sub>O<sub>2</sub>.

role of gallic and cinnamic acid anti-oxidative mechanism and inhibition of H<sup>+</sup>,K<sup>+</sup>-ATPase of *H. pylori*<sup>52</sup>. Yet, future mechanistic studies must be performed to understand how AntiOxBEN<sub>3</sub> desensitises mPTP, including possible effects on the ATP synthase.

#### Cytotoxicity of AntiOxBEN<sub>3</sub> on HepG2 cells

AntiOxBEN<sub>3</sub> cytotoxic profile was assessed<sup>19</sup> on a human hepatocellular carcinoma cell line (HepG2), an *in vitro* system often used in toxicological studies. From the cytotoxicity data (IC<sub>50</sub> = 254  $\pm$  32  $\mu$ M), it can be concluded that AntiOxBEN<sub>3</sub> presented low cellular toxicity (Figure 5(A)) having a promising safety margin for clinical use. Concurrently, a new mitochondriotropic compound based on gallic acid was developed by Jara et al.<sup>34</sup> aiming to disrupt mitochondrial functioning in tumour cells by a mechanism similar to the one proposed for gallic acid ester derivatives. Antioxidants can be seen as a double-edged sword as they can also act as pro-oxidants in a diversity of systems based on its structure, concentration, and cellular redox context<sup>53</sup>. The TPP-gallic acid ester derivative (TPP + C12) is very toxic for different tumour cell lines (IC<sub>50</sub> = 1  $\mu$ M)<sup>34</sup>, while AntiOxBEN<sub>3</sub> (having 12 carbons and two peptide bonds) showed lower toxicity towards HepG2 cells (IC<sub>50</sub> = 250  $\mu$ M). The type of spacer linking gallic acid and the TPP moiety differs between these two mitochondria-targeted molecules, suggesting that presence of an ester bond potentiate cytotoxicity effects. Moreover, the previously described mitochondriotropic agents based on gallic acid are toxic and can be easily hydrolysed by esterases limiting the administration route and biological usefulness.

#### AntiOxBEN<sub>3</sub> antioxidant effects on HepG2 cells

HepG2 cells were then incubated with different inducers of oxidative stress (250  $\mu$ M FeSO<sub>4</sub> and 250  $\mu$ M H<sub>2</sub>O<sub>2</sub>). The oxidant stressor resulted into a significant inhibition of cell proliferation when compared with control. Yet, pre-treating cells with AntiOxBEN<sub>3</sub> significantly prevented iron- and hydrogen peroxide-induced HepG2 cytotoxicity (Figure 5(B)). From this and previous data, esterification of carboxylic group and length of the linker seems to potentiate hydroxybenzoic acids cytotoxicity<sup>34,35</sup> while peptide-like bond, present in AntiOxBENs, potentiate antioxidant activity<sup>17</sup>. Jara et al. reported that TPP-gallic acid ester derivatives (TPP + C8–12)

presented cytotoxic effects on different tumour cell lines at the low micromolar range (1–10  $\mu$ M)<sup>34</sup>, although AntiOxBEN<sub>3</sub> (100  $\mu$ M) presented effective antioxidant activity towards Fe/H<sub>2</sub>O<sub>2</sub> (250  $\mu$ M/250  $\mu$ M) in a hepatocarcinoma cell line. Furthermore, Jara et al. reported that TPP + C8–12 induced mPTP opening in cells<sup>34</sup>, while AntiOxBEN<sub>3</sub> prevented the Ca<sup>2+</sup>-induced mPTP opening in isolated mitochondrial fractions. Once again, only the type of spacer linking gallic acid and the TPP moiety differs between these two mitochondria-targeted molecules. Herein, we pointed out that the driving force on cytotoxic effects of mitochondria-targeted gallic acid derivatives may not be the aromatic ring pattern substitution. Actually, in the AntiOxBEN<sub>3</sub> molecule, the spacer is linked to gallic acid and TPP moiety by two peptide-like bonds making this mitochondriotropic antioxidant less toxic and more stable on biological systems.

#### Conclusion

This work highlights the successful development of a new mitochondriotropic antioxidant based on gallic acid that efficiently transports gallic acid to mitochondria without disturbing mitochondrial function and with distinct iron-chelation and antioxidant properties overcoming gallic acid bioavailability drawbacks. AntiOxBEN<sub>3</sub> low cytotoxicity profile allows its use in the prevention of mitochondrial oxidative damage and in the regulation of oxidative stress pathways. Additionally, it was shown that this type of mitochondriotropic antioxidants can prevent calcium-dependent mPTP opening. So, AntiOxBEN<sub>3</sub> can be considered a promising lead compound for the development of a new class of mPTP inhibitors to be used as mPTP de-sensitiser for basic research or clinical applications or undergo an optimisation programme from which a new drug based on gallic acid can emerge for therapeutic application in mitochondria dysfunction-related disorders.

#### Disclosure statement

The authors report no declarations of interest. Still, all the authors would like to mention that all the compounds, processes, and applications are under patent (NPAT260). PJO and FB are co-founders of CNC/UP spin-off company MitoTAG.





## Funding

This project was supported by Foundation for Science and Technology (FCT) and FEDER/COMPETE [Grants POCI-01-0145-FEDER-007440, POCI-01-0145-FEDER-016659, UID/QUI/00081/2013/POCI-01-0145-FEDER-006980, PTDC/DTP-FTO/2433/2014, and NORTE-01-0145-FEDER-000028]. J Teixeira, C Oliveira, and F. Cagide were supported by grants from FCT, POPH, FEDER/COMPETE, and Norte2020. Ricardo Amorim is recipient of a Ph.D. fellowship from the FCT [SFRH/BD/131070/2017].

## ORCID

José Teixeira  <http://orcid.org/0000-0003-0834-5698>

Fernanda Borges  <http://orcid.org/0000-0003-1050-2402>

Paulo J. Oliveira  <http://orcid.org/0000-0002-5201-9948>

## References

- Brand MD, Nicholls DG. Assessing mitochondrial dysfunction in cells. *Biochem J* 2011;435:297–312.
- Smith RA, Hartley RC, Cocheme HM, Murphy MP. Mitochondrial pharmacology. *Trends Pharm Sci* 2012;33:341–52.
- James AM, Collins Y, Logan A, Murphy MP. Mitochondrial oxidative stress and the metabolic syndrome. *Trends Endocrinol Metab* 2012;23:429–34.
- Terman A, Dalen H, Eaton JW, et al. Aging of cardiac myocytes in culture: oxidative stress, lipofuscin accumulation, and mitochondrial turnover. *Ann NY Acad Sci* 2004;1019:70–7.
- Edeas M, Weissig V. Targeting mitochondria: strategies, innovations and challenges: the future of medicine will come through mitochondria. *Mitochondrion* 2013;13:389–90.
- Rohlena J, Dong LF, Neuzil J. Targeting the mitochondrial electron transport chain complexes for the induction of apoptosis and cancer treatment. *Curr Pharm Biotechnol* 2013;14:377–89.
- Murphy MP, Smith RA. Targeting antioxidants to mitochondria by conjugation to lipophilic cations. *Ann Rev Pharmacol Toxicol* 2007;47:629–56.
- Andreux PA, Houtkooper RH, Auwerx J. Pharmacological approaches to restore mitochondrial function. *Nat Rev Drug Discov* 2013;12:465–83.
- Parikh S, Saneto R, Falk MJ, et al. A modern approach to the treatment of mitochondrial disease. *Curr Treat Options Neurol* 2009;11:414–30.
- Apostolova N, Victor VM. Molecular strategies for targeting antioxidants to mitochondria: therapeutic implications. *Antioxid Redox Signal* 2015;22:686–729.
- Benfeito S, Oliveira C, Soares P, et al. Antioxidant therapy: still in search of the ‘magic bullet’. *Mitochondrion* 2013;13:427–35.
- Badhani B, Sharma N, Kakkar R. Gallic acid: a versatile antioxidant with promising therapeutic and industrial applications. *RSC Adv* 2015;5:27540–57.
- Fazary AE, Taha M, Ju YH. Iron complexation studies of gallic acid. *J Chem Eng Data* 2009;54:35–42.
- Wu S, Cao Q, Wang X, et al. Design, synthesis and biological evaluation of mitochondria targeting theranostic agents. *Chem Commun (Camb)* 2014;50:8919–22.
- Teixeira J, Soares P, Benfeito S, et al. Rational discovery and development of a mitochondria-targeted antioxidant based on cinnamic acid scaffold. *Free Radic Res* 2012;46:600–11.
- Smith RA, Murphy MP. Mitochondria-targeted antioxidants as therapies. *Discov Med* 2011;11:106–14.
- Teixeira J, Oliveira C, Amorim R, et al. Development of hydroxybenzoic-based platforms as a solution to deliver dietary antioxidants to mitochondria. *Sci Rep* 2017;7:6842.
- Teixeira J, Cagide F, Benfeito S, et al. Development of a mitochondriotropic antioxidant based on caffeic acid: proof of concept on cellular and mitochondrial oxidative stress models. *J Med Chem* 2017;60:7084–98.
- Serafim TL, Carvalho FS, Marques MP, et al. Lipophilic caffeic and ferulic acid derivatives presenting cytotoxicity against human breast cancer cells. *Chem Res Toxicol* 2011;24:763–74.
- Gornall AG, Bardawill CJ, David MM. Determination of serum proteins by means of the biuret reaction. *J Biol Chem* 1949;177:751–66.
- Asin-Cayuela J, Manas AR, James AM, et al. Fine-tuning the hydrophobicity of a mitochondria-targeted antioxidant. *FEBS Lett* 2004;571:9–16.
- Akerman KE, Wikstrom MK. Safranin as a probe of the mitochondrial membrane potential. *FEBS Lett* 1976;68:191–7.
- Kowaltowski AJ, Castilho RF. Ca<sup>2+</sup> acting at the external side of the inner mitochondrial membrane can stimulate mitochondrial permeability transition induced by phenylarsine oxide. *Biochim Biophys Acta* 1997;1322:221–9.
- Soriano ME, Nicolosi L, Bernardi P. Desensitization of the permeability transition pore by cyclosporin a prevents activation of the mitochondrial apoptotic pathway and liver damage by tumor necrosis factor-alpha. *J Biol Chem* 2004;279:36803–8.
- Corominas-Faja B, Santangelo E, Cuyas E, et al. Computer-aided discovery of biological activity spectra for anti-aging and anti-cancer olive oil oleuropeins. *Aging* 2014;6:731–41.
- Biasutto L, Mattarei A, Marotta E, et al. Development of mitochondria-targeted derivatives of resveratrol. *Bioorg Med Chem Lett* 2008;18:5594–7.
- Mattarei A, Biasutto L, Marotta E, et al. A mitochondriotropic derivative of quercetin: a strategy to increase the effectiveness of polyphenols. *Chembiochem* 2008;9:2633–42.
- Reddy CA, Somepalli V, Golakoti T, et al. Mitochondria-targeted curcuminoids: a strategy to enhance bioavailability and anticancer efficacy of curcumin. *PLoS One* 2014;9:e89351.
- Jayakumar S, Patwardhan RS, Pal D, et al. Mitochondria targeted curcumin exhibits anticancer effects through disruption of mitochondrial redox and modulation of TrxR2 activity. *Free Radic Biol Med* 2017;113:530–8.
- Sassi N, Biasutto L, Mattarei A, et al. Cytotoxicity of a mitochondriotropic quercetin derivative: mechanisms. *Biochim Biophys Acta* 2012;1817:1095–106.
- Sassi N, Mattarei A, Azzolini M, et al. Mitochondria-targeted resveratrol derivatives act as cytotoxic pro-oxidants. *Curr Pharm Des* 2014;20:172–9.
- Kamo N, Muratsugu M, Hongoh R, Kobatake Y. Membrane potential of mitochondria measured with an electrode sensitive to tetraphenyl phosphonium and relationship between proton electrochemical potential and phosphorylation potential in steady state. *J Memb Biol* 1979;49:105–21.
- Antonenko YN, Avetisyan AV, Cherepanov DA, et al. Derivatives of rhodamine 19 as mild mitochondria-targeted cationic uncouplers. *J Biol Chem* 2011;286:17831–40.

34. Jara JA, Castro-Castillo V, Saavedra-Olavarria J, et al. Antiproliferative and uncoupling effects of delocalized, lipophilic, cationic gallic acid derivatives on cancer cell lines. Validation in vivo in syngenic mice. *J Med Chem* 2014;57:2440–54.
35. Cortes LA, Castro L, Pesce B, et al. Novel gallate triphenylphosphonium derivatives with potent antichagasic activity. *PLoS One* 2015;10:e0136852.
36. Biasutto L, Sassi N, Mattarei A, et al. Impact of mitochondriotropic quercetin derivatives on mitochondria. *Biochim Biophys Acta* 2010;1797:189–96.
37. Lane DJ, Merlot AM, Huang ML, et al. Cellular iron uptake, trafficking and metabolism: key molecules and mechanisms and their roles in disease. *Biochim Biophys Acta* 2015;1853:1130–44.
38. Andjelković M, Van Camp J, De Meulenaer B, et al. Iron-chelation properties of phenolic acids bearing catechol and galloyl groups. *Food Chem* 2006;98:23–31.
39. Perron NR, Brumaghim JL. A review of the antioxidant mechanisms of polyphenol compounds related to iron binding. *Cell Biochem Biophys* 2009;53:75–100.
40. Reckziegel P, Dias VT, Benvegna DM, et al. Antioxidant protection of gallic acid against toxicity induced by Pb in blood, liver and kidney of rats. *Toxicol Report* 2016;3:351–6.
41. Stanely Mainzen Prince P, Priscilla H, Devika PT. Gallic acid prevents lysosomal damage in isoproterenol induced cardiotoxicity in Wistar rats. *Eur J Pharm* 2009;615:139–43.
42. Bernardi P, Rasola A, Forte M, Lippe G. The mitochondrial permeability transition pore: channel formation by F-ATP synthase, integration in signal transduction, and role in pathophysiology. *Physiol Rev* 2015;95:1111–55.
43. Nakagawa Y, Moore G. Role of mitochondrial membrane permeability transition in p-hydroxybenzoate ester-induced cytotoxicity in rat hepatocytes. *Biochem Pharmacol* 1999;58:811–6.
44. Haouzi D, Cohen I, Vieira HL, et al. Mitochondrial permeability transition as a novel principle of hepatorenal toxicity in vivo. *Apoptosis* 2002;7:395–405.
45. Rao VK, Carlson EA, Yan SS. Mitochondrial permeability transition pore is a potential drug target for neurodegeneration. *Biochim Biophys Acta* 2014;1842:1267–72.
46. Ong SB, Samangouei P, Kalkhoran SB, Hausenloy DJ. The mitochondrial permeability transition pore and its role in myocardial ischemia reperfusion injury. *J Mol Cell Cardiol* 2015;78:23–34.
47. Assaly R, de Tassigny A, Paradis S, et al. Oxidative stress, mitochondrial permeability transition pore opening and cell death during hypoxia-reoxygenation in adult cardiomyocytes. *Eur J Pharmacol* 2012;675:6–14.
48. Sandmann BJ, Chien MH, Sandmann RA. Stability constants of calcium, magnesium and zinc gallate using a divalent ion-selective electrode. *Anal Lett* 1985;18:149–59.
49. Sun J, Ren DD, Wan JY, et al. Desensitizing mitochondrial permeability transition by ERK-cyclophilin D axis contributes to the neuroprotective effect of gallic acid against cerebral ischemia/reperfusion injury. *Fron Pharmacol* 2017;8:184.
50. Hong S, Pedersen PL. ATP synthase and the actions of inhibitors utilized to study its roles in human health, disease, and other scientific areas. *Microbiol Mol Biol Rev* 2008;72:590–641.
51. Ahmad Z, Laughlin TF. Medicinal chemistry of ATP synthase: a potential drug target of dietary polyphenols and amphibian antimicrobial peptides. *Curr Med Chem* 2010;17:2822–36.
52. Nanjundaiah SM, Annaiah HN, Dharmesh SM. Gastroprotective effect of ginger rhizome (*Zingiber officinale*) extract: role of gallic acid and cinnamic acid in H(+), K(+)-ATPase/H. pylori Inhibition and anti-Oxidative Mechanism. *Evid Based Complement Alternat Med* 2011;2011:249487.
53. Bouayed J, Bohn T. Exogenous antioxidants—double-edged swords in cellular redox state: health beneficial effects at physiologic doses versus deleterious effects at high doses. *Oxid Med Cell Longev* 2010;3:228–37.